DTIC
S **ELECTE**
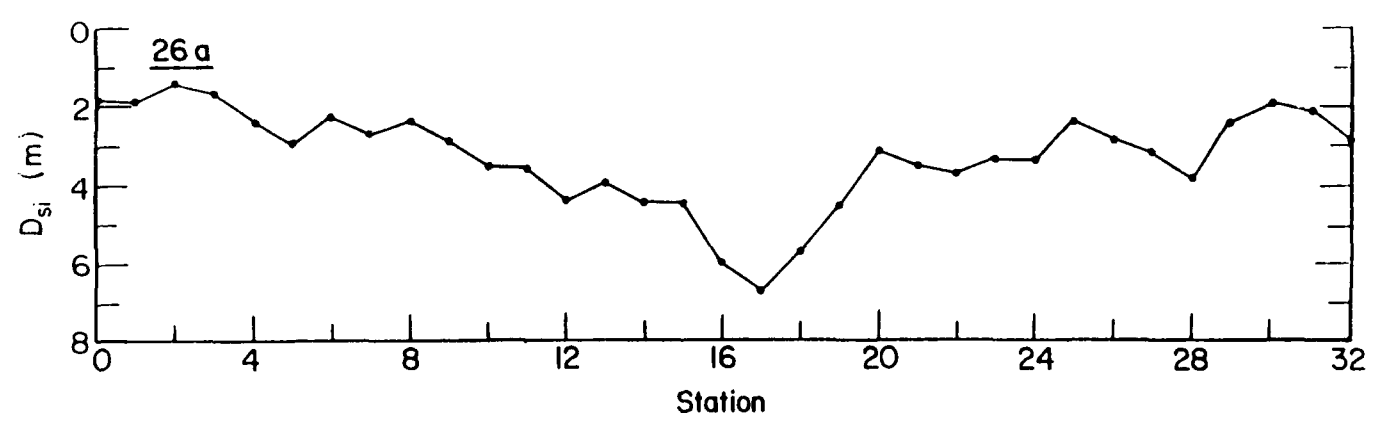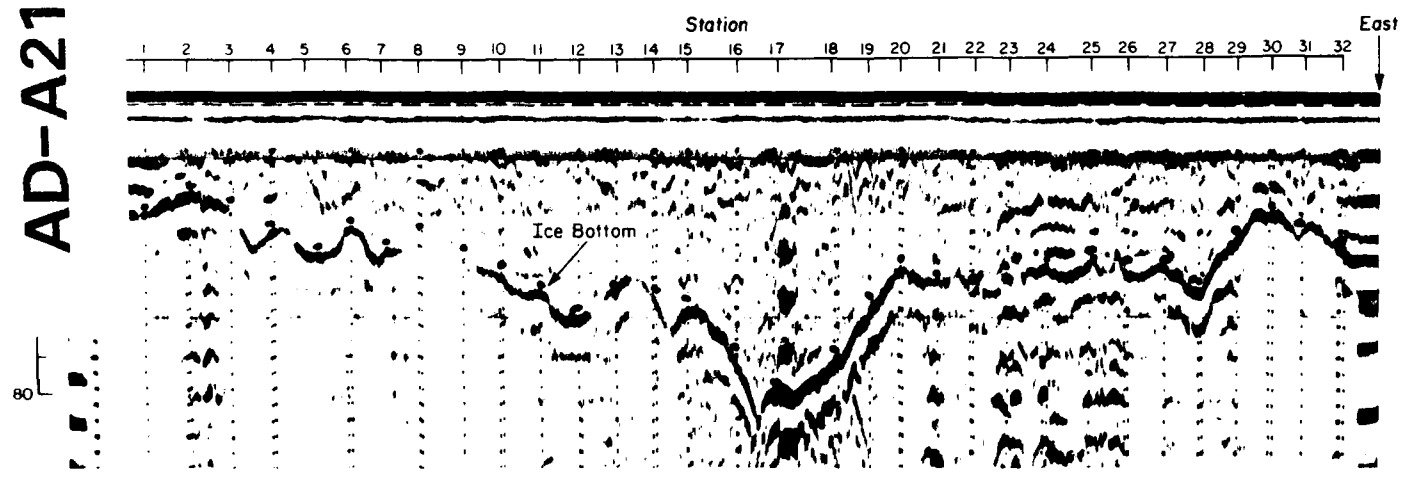FEB 1 5 1990
D
D a

(4)

US Army Corps of Engineers
Cold Regions Research & Engineering Laboratory

Estimating sea ice thickness using time-of-flight data from impulse radar soundings
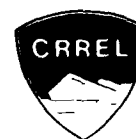
AD-A218 736

90 02 14 053

For conversion of SI metric units to U.S./British customary units of measurement consult ASTM Standard E380, Metric Practice Guide, published by the American Society for Testing and Materials, 1916 Race St., Philadelphia, Pa. 19103.

Cover: Graphic record of radar sounding profile taken with 80-MHz antenna (top) and associated profile determined from drill holes.

CRREL Report 89-22

December 1989

Estimating sea ice thickness using time-of-flight data from impulse radar soundings

Austin Kovacs and Rexford M. Morey

REPORT DOCUMENTATION PAGE

1a. REPORT SECURITY CLASSIFICATION	1B. RESTRICTIVE MARKINGS
Unclassified	

2a. SECURITY CLASSIFICATION AUTHORITY	3. DISTRIBUTION/AVAILABILITY OF REPORT
2b. DECLASSIFICATION/DOWNGRADING SCHEDULE	Approved for public release; distribution is unlimited.

4. PERFORMING ORGANIZATION REPORT NUMBER(S)	5. MONITORING ORGANIZATION REPORT NUMBER(S)
CRREL Report 89-22	

6a. NAME OF PERFORMING ORGANIZATION	6b. OFFICE SYMBOL (if applicable)	7a. NAME OF MONITORING ORGANIZATION
U.S. Army Cold Regions Research and Engineering Laboratory	CECRL	Naval Oceanographic and Atmospheric Research Laboratory

6c. ADDRESS (City, State, and ZIP Code)	7b. ADDRESS (City, State, and ZIP Code)
72 Lyme Road Hanover, N.H. 03755-1290	Stennis Space Center Mississippi 39529-5004

8a. NAME OF FUNDING/SPONSORING ORGANIZATION	8b. OFFICE SYMBOL (if applicable)	9. PROCUREMENT INSTRUMENT IDENTIFICATION NUMBER
		Contract N6845286MP6003, Program Element 63704

8c. ADDRESS (City, State, and ZIP Code)	10. SOURCE OF FUNDING NUMBERS			
	PROGRAM ELEMENT NO.	PROJECT NO.	TASK NO.	WORK UNIT ACCESSION NO.

11. TITLE (Include Security Classification)

Estimating Sea Ice Thickness Using Time-of-Flight Data from Impulse Radar Soundings

12. PERSONAL AUTHOR(S)
Kovacs, Austin and Morey, Rexford M.

13a. TYPE OF REPORT	13b. TIME COVERED FROM _____ TO _____	14. DATE OF REPORT (Year, Month, Day) December 1989	15. PAGE COUNT 13

16. SUPPLEMENTARY NOTATION

17. COSATI CODES			18. SUBJECT TERMS (Continue on reverse if necessary and identify by block number)
FIELD	GROUP	SUB-GROUP	Field studies
			Impulse radar soundings
			Radar

Field studies · Sea ice
Impulse radar soundings · Sea ice thickness
Radar

19. ABSTRACT (Continue on reverse if necessary and identify by block number)

Two second-year sea ice floes were probed using "impulse" radar sounding and direct drilling methods. The resulting two-way time of flight of the impulse radar EM wavelet, traveling from the surface to the ice "bottom" and back to the surface, was compared with snow and ice thickness data obtained from a drill hole. From this comparison, simple relationships are presented that provide an estimate of the thickness of sea ice, from about 1 to 8 m thick, with or without a snow cover. Relations are also presented that show the bulk or apparent dielectric constant of the ice floes vs ice thickness, again with or without the snow cover. The data revealed that the apparent dielectric constant of the sea ice decreased with increasing ice thickness from a value of about 7 for ice 1 m thick to about 3.5 for ice 6 m thick.

20. DISTRIBUTION/AVAILABILITY OF ABSTRACT	21. ABSTRACT SECURITY CLASSIFICATION
[X] UNCLASSIFIED/UNLIMITED ☐ SAME AS RPT. ☐ DTIC USERS	Unclassified

22a. NAME OF RESPONSIBLE INDIVIDUAL	22b. TELEPHONE (Include Area Code)	22c. OFFICE SYMBOL
Austin Kovacs	603-646-4100	CECRL-EA

DD FORM 1473, 84 MAR

83 APR edition may be used until exhausted.
All other editions are obsolete.

PREFACE

The contents of this report are not to be used for advertising or promotional purposes. Citation of brand names does not constitute an official endorsement or approval of the use of such commercial products.

Estimating Sea Ice Thickness Using Time-of-Flight Data From Impulse Radar Soundings

AUSTIN KOVACS AND REXFORD M. MOREY

INTRODUCTION

The remote measurement of sea ice thickness using impulse radar has been actively pursued for some time. However, sea ice is a complex, lossy dielectric consisting of pure ice, liquid brine and air, and these properties vary with ice thickness, temperature and time. Knowledge of the bulk dielectric constant (E) of sea ice, therefore, forms the basis for the measurement of its thickness, since the velocity of the impulse radar electromagnetic (EM) wavelet in the ice is directly related to E.

If one knows the bulk dielectric constant of the sea ice (at the radar sounding frequency), then the velocity of the EM wavelet in the ice can be determined, and, if the transit time of the wavelet from the surface to the ice bottom and back is measured by an impulse radar system, then the ice thickness can be estimated. Unfortunately, the dielectric constant of the sea ice is generally not known and some "representative" value is assumed that can lead to a poor estimate of the EM wavelet velocity and, therefore, ice thickness determination.

In this report we present the results of over 225 drill hole measurements to determine sea ice thickness and snow depth. These measurements were correlated with impulse radar sounding data to develop simple relations between the impulse radar EM wavelet two-way travel time and the snow plus sea ice thickness and the sea ice thickness.

FIELD MEASUREMENTS

Two second-year sea ice floes were studied to determine their snow and ice thickness variation and the two-way time of flight of an impulse radar EM wavelet traveling from the surface to the ice "bottom" and back to the surface. The measurements included impulse radar profiles made on the surface and from a helicopter. A Geophysical Survey Systems, Inc., impulse radar system was used.

On one sea ice floe, the company's designated 80-MHz antenna was used, and on the second floe, their designated 120-MHz antenna was used. The actual free-space center frequencies of the broadband wavelet spectra transmitted by these antennas are about 50% higher than their designated values, but they decrease as a result of antenna loading effects associated with antenna–surface coupling. Since ice and snow surface conditions varied across the floes, the center frequency of the wavelet spectra also varied. This variation was not determined. Therefore, in this report, sounding results are referenced to the manufacturers designated antenna frequency.

The first ice floe, located north of Prudhoe Bay, Alaska, was studied the first week of May 1985 when air temperatures were between –15 and –20°C. On this floe, three parallel lines, about 240 m long and 11.5 m apart, were established. Along each line, radar sounding profiles were made and snow, D_s, and ice, D_i, thicknesses were tape-measured. The center of the lines crossed over a small pressure ridge (Fig. 1a). Ice thickness was determined by use of an electric drill powering a 5-cm-diameter continuous-auger flight system. With a generator, this system, with ten 1-m-long stainless steel auger flights, weighed about 60 kg. On average, about 70 m of ice was drilled per hour. This time included drilling, tape measurement of ice thickness, and relocation of equipment to the next drill site. These sites were spaced about 7.5 m apart along each of the three lines, as shown in Figure 1b.

The second ice floe was studied in late April 1987 when air temperatures were also between –15 and –20°C. This floe was located northwest of Prudhoe Bay. On this floe, radar sounding and snow and ice thickness measurements were made at random locations. Ice thickness measurements were made using a tape lowered through holes bored in the ice by a hot-water drilling system. This system weighed about 240 kg and consisted of a small oil-fired boiler, a high-pressure pump, a generator and a
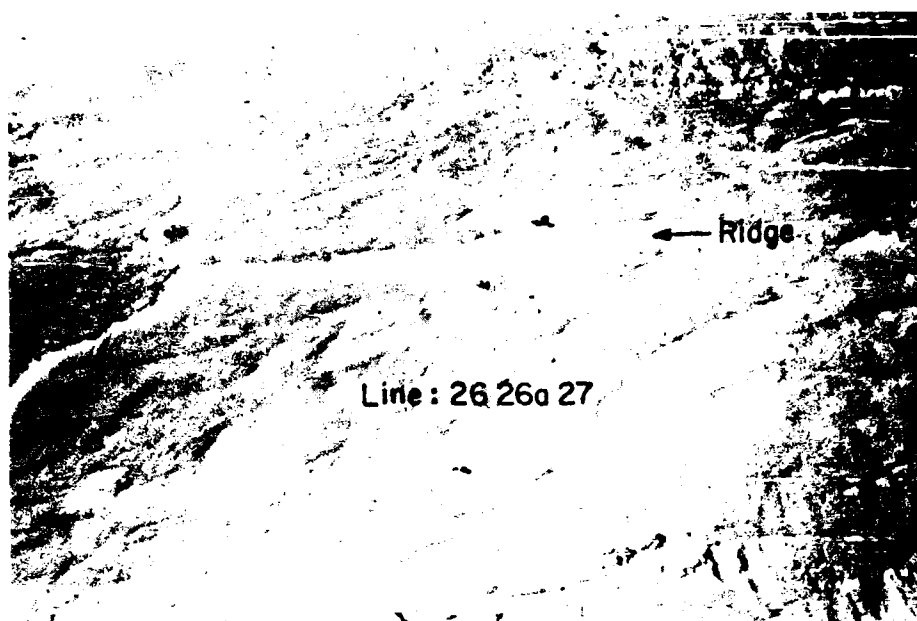
a. Aerial view.
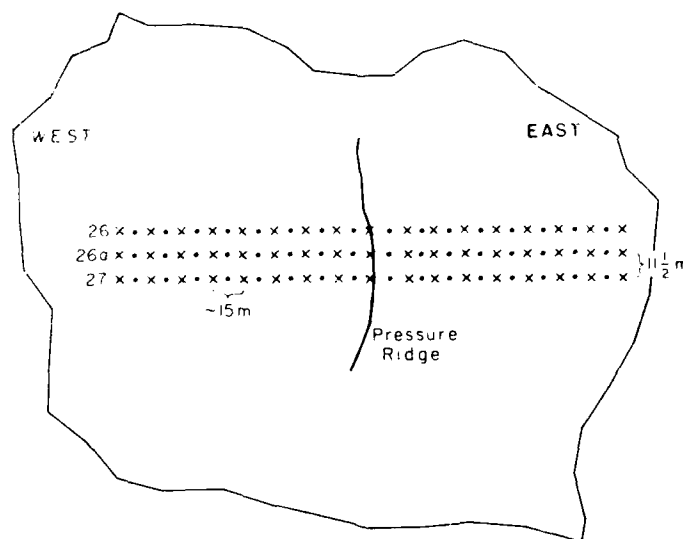
b. Survey tracks along which radar sounding were made.

Figure 1. Ice floe studied in 1985.

hose reel with 60 m of hose. The drill probe consisted of a hollow, 1-m-long, 2.5-cm-diameter brass rod with a tapered end. Water exited at the probe tip through a hole about 63 mm in diameter. Seawater was heated and used as the drilling fluid. With 55 m of hose resting on the ice, the temperature of the water at the probe tip was about 45°C. In a 4-hour period, with air temperatures at –18°C, the hot-water drill we used melted holes through ice having an average thickness of 4.9 m at an average rate of 1.75 m/min. This rate included the short time required to move the hose and probe from one site to the next and measure the snow and ice thickness. Each site was 5 m from the previous one. As with the mechanical auger flight system, the hot-water drilling was a two-man operation.

2

Table 1. Radar and thickness information from the 80-MHz antenna for the ice floe studied in 1985.

| Station no.	Time in snow and ice (ns)	Ice thickness (m)	Snow and ice thickness (m)	Snow and ice apparent dielectric constant E_{dsi}	Station no.	Time in snow and ice (ns)	Ice thickness (m)	Snow and ice thickness (m)	Snow and ice apparent dielectric constant E_{dsi}
27-2	25.0	1.60	1.70	4.87	26-a26	44.5	3.25	3.30	4.09
27-3	26.0	1.70	1.75	4.97	27-0	44.5	3.40	3.60	3.44
27-4	26.5	1.75	1.85	4.62	27-30	45.5	3.41	3.50	3.80
26-a3	27.0	1.58	1.85	4.79	27-11	45.5	3.57	3.65	3.50
26-a0	28.0	1.78	1.85	5.15	27-28	45.5	3.71	3.80	3.23
26-0	28.5	1.71	2.00	4.57	27-26	45.5	3.42	3.50	3.80
26-a30	29.0	1.95	2.00	4.73	26-a23	45.5	3.13	3.60	3.59
27-7	29.0	1.97	2.15	4.09	26-22	46.0	3.63	3.70	3.48
26-a1	29.5	1.88	2.00	4.90	26-7	47.0	3.52	3.70	3.63
26-5	30.0	2.06	2.10	4.59	26-21	47.0	3.62	3.70	3.63
26-4	33.5	2.27	2.45	4.21	27-20	47.0	3.30	3.85	3.35
26-a31	34.0	2.06	2.30	4.92	26-9	47.0	3.58	3.65	3.73
26-a4	34.5	2.25	2.45	4.46	26-18	47.0	3.38	3.80	3.44
26-a6	34.5	2.12	2.50	4.28	26-a10	47.0	3.50	3.60	3.84
26-a8	35.0	2.31	2.50	4.41	26-a21	47.5	3.51	3.60	3.92
26-25	35.0	2.34	2.60	4.08	26-20	47.5	3.77	3.80	3.52
26-a29	35.5	2.43	2.65	4.04	27-21	48.0	3.79	3.85	3.50
26-1	35.5	2.50	2.60	4.19	26-8	48.5	3.63	3.70	3.87
27-25	35.5	2.31	2.70	3.89	26-a22	49.0	3.67	3.75	3.84
27-24	36.5	2.55	2.75	3.96	26-11	49.0	3.40	3.60	4.17
26-26	39.0	2.94	3.00	3.80	26-a28	50.5	3.82	3.90	3.77
27-22	39.0	2.76	3.10	3.56	26-a13	50.5	3.93	4.00	3.59
26-a32	39.0	2.81	2.90	4.07	27-14	51.0	3.87	4.00	3.66
27-13	39.0	2.73	2.85	4.21	27-29	51.0	4.16	4.25	3.21
26-a7	39.0	2.50	2.90	4.07	26-a11	51.5	3.62	4.00	3.73
26-31	39.0	2.79	2.90	4.07	27-19	52.0	3.76	4.00	3.80
26-29	40.0	2.94	3.05	3.87	26-19	52.0	4.21	4.30	3.29
27-32	40.0	2.72	3.10	3.75	27-15.5	54.0	3.93	4.45	3.31
26-6	40.0	2.71	3.10	3.75	26-12	54.0	4.11	4.20	3.72
27-31	40.0	2.85	3.00	4.00	26-15	54.5	4.12	4.55	3.23
26-30	40.0	3.07	3.25	3.41	26-a14	55.0	4.32	4.60	3.22
27-27	40.0	2.77	3.20	3.52	26-a12	57.0	4.37	4.45	3.69
26-a25	40.5	2.71	3.20	3.60	26-14	58.0	4.64	4.70	3.43
26-a9	41.0	2.75	3.00	4.20	26-a15	58.0	4.20	4.70	3.43
27-10	41.0	3.14	3.20	3.69	26-2	58.0	4.43	4.55	3.66
26-27	41.0	3.13	3.25	3.58	26-17	59.0	4.55	4.95	3.20
26-a5	41.0	2.97	3.05	4.07	26-a13	59.0	4.51	4.60	3.70
26-32	41.0	3.23	3.30	3.47	26-a14.5	63.0	4.80	5.20	3.30
26-3	42.0	3.02	3.50	3.24	27-18	63.0	4.84	5.05	3.50
27-12	42.5	2.97	3.10	4.23	26-a15.5	64.0	4.59	5.05	3.61
27-9	42.5	3.23	3.30	3.73	26-a18	72.0	5.59	5.80	3.47
27-23	43.0	3.19	3.30	3.82	26-a16	73.5	5.95	6.05	3.52
26-28	43.0	3.18	3.25	3.94	26-16	74.5	6.06	6.10	3.36
26-10	43.0	2.98	3.20	4.06	27-17	76.5	5.99	6.20	3.43
26-a27	43.0	3.07	3.30	3.82	27-17.5	78.0	6.05	6.20	3.56
26-a24	43.0	2.99	3.40	3.60	26-a17.5	80.0	6.29	6.60	3.31
27-8	43.5	3.30	3.40	3.68	27-16.5	83.0	6.35	6.65	3.51
26-24	44.0	3.41	3.50	3.56	26-a17	84.0	6.61	6.90	3.33
26-23	44.0	3.45	3.50	3.56	26-a16.5	91.0	7.65	7.70	3.14
26-a28	44.5	3.07	3.35	3.97					

3
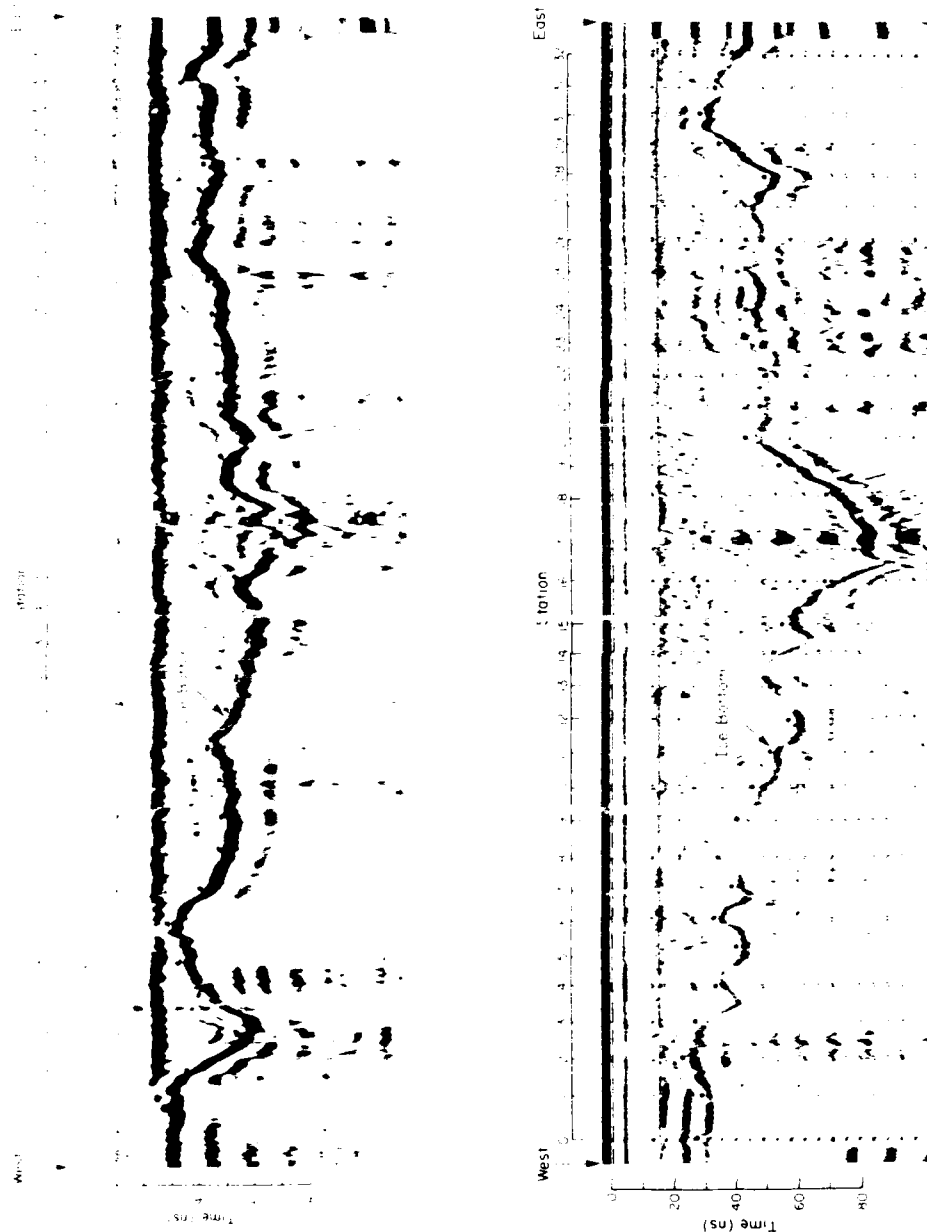
Figure 2. Graphic record of radar sounding profiles taken in 1985 with the 80-MHz antenna along lines 2o (top record) and 26a (bottom record).

4

RESULTS

In 1985, radar profiles along each of the three lines shown in Figure 1 were made by dragging the 80-MHz antenna on the surface. The graphic records of the two-way EM wavelet travel times obtained along line 26 and 26a are presented in Figure 2. Only one voltage polarity was printed to highlight the reflection from the ice "bottom" and to aid in picking the two-way time of travel, T_{si}, of the transmitted EM wavelet from the antenna on the surface, through the snow, to the "bottom" of the ice, and then back to the antenna. Since the antenna was pulled along the surface, the travel time includes the wavelet propagation time through the snowcover, where it existed, as well as in the ice. Cross sections of the snow and ice thickness measured along lines 26 and 26a are presented in Figure 3. Figures 2 and 3 reveal similar profile variations.

The EM wavelet travel time in the snow and ice at each station is listed, in ascending order, in Table 1. Also listed are the ice and the snow plus ice thicknesses, and the calculated apparent dielectric constants for the combined snow plus ice thickness, E_{asi}, at each station. E_{asi} was determined from $E_{asi} = (T_{si} \times C/2 D_{si})^2$, where $C = 0.3$ m ns^{-1} and D_{si} is the snow–ice thickness. E_{asi} represents a bulk electrical property that controls the effective speed at which the EM wavelet travels in the medium.

A similar presentation of the data collected in 1987 with the 120-MHz antenna is given in Table 2. The ice thickness at each station is also listed in Table 2 along with the relative apparent dielectric constant of the ice, E_{ai}, as determined by $E_{ai} = (T_{si} \times C/2 D_i)^2$.

In most ground-based or airborne radar sounding surveys of sea ice thickness, the goal is to estimate the ice thickness from the EM wavelet two-way travel times. The snow cover is generally not of interest, but is frequently present on winter ice. To aid in the above goal, plots of D_{si} vs T_{si} are shown in Figure 4 for the 1985 and 1987 data. There may be a slight bias in the data of less than 1 ns. This bias would be caused by system timing inaccuracies. Another reason for a time bias is that the EM wavelet was not reflected from the ice/water boundary, the tape-measured interface depth, but from a moist zone interface about 5 cm above the ice bottom (Kovacs et al. 1987). Linear and power regression curves were fitted to the data. Both curves have nearly identical correlation coefficients. The power curve is more realistic since it shows that the time is zero when the thickness is zero. Also, the linear curve indicates that the ratio D_{si}/T_{si} is a constant, which implies that the bulk dielectric constant, E_{asi}, is a constant independent of sea ice thickness. Younger, thinner sea ice has a higher dielectric constant, E_{ai}, than older, thicker sea ice since there is proportionately more brine vs depth in thinner sea ice, which retards EM wavelet propagation (Kovacs et al. 1987). Therefore, D_{si}/T_{si} cannot be a constant. However, the reason for including the straight line curves is that they represent simple equations for estimating the thickness of winter sea ice from the measured EM wavelet two-way travel time in ice between about 1 and 8 m thick. In addition, use of the linear curves provides thinner and, therefore, more conservative estimates for ice between about 1 and 2 m thick, a range of practical concern for certain over-ice travel.

The slopes of the linear regression lines passing through the data in Figure 4 are the same, but there is a slight vertical offset. Statistically, this offset is not significant, since the line for one data set falls well within the standard deviation of the other. Nevertheless, the offset is related to differences in
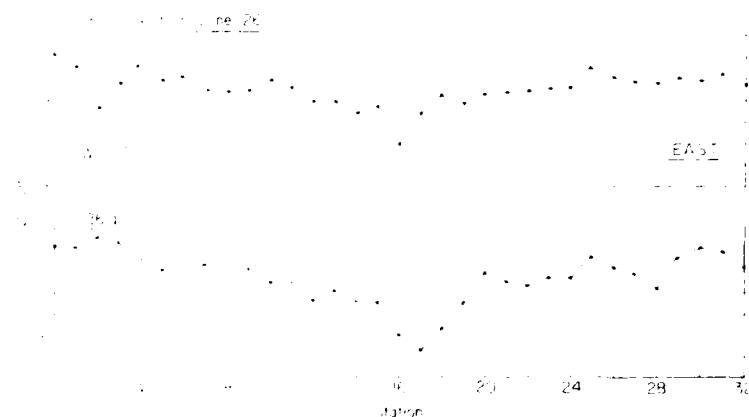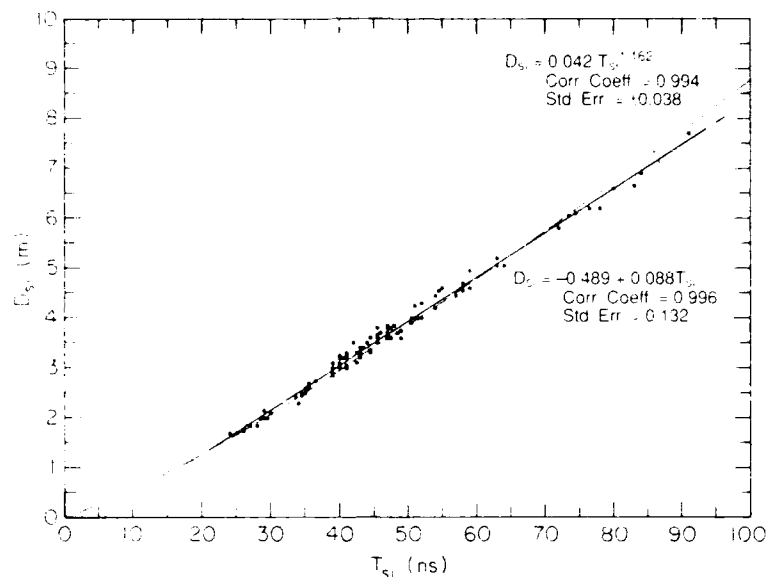

Figure 3. Snow and ice thickness, D_{si}, along tracks 26 and 26a profiled in 1985 with the 80-MHz antenna.

5

Table 2. Radar and thickness information from the 120-MHz antenna for the ice floe studied in 1987.

Station no.	Time in snow and ice (ns)	Ice thickness (m)	Snow and ice thickness (m)	Snow and ice apparent dielectric constant E_{asi}	Ice apparent dielectric constant E_{ii}	Station no.	Time in snow and ice (ns)	Ice thickness (m)	Snow and ice thickness (m)	Snow and ice apparent dielectric constant E_{asi}	Ice apparent dielectric constant E_{ii}
lead	10.0	0.55	0.55	7.44	7.44	E-32	55.0	4.01	4.20	3.86	4.23
lead	17.0	0.95	0.95	7.20	7.20	C-25	55.0	4.12	4.27	3.73	4.01
lead	23.0	1.45	1.45	5.66	5.66	E-38	55.0	4.19	4.22	3.82	3.88
C-47	25.0	1.60	1.82	4.24	5.49	E-33	55.0	4.21	4.28	3.85	3.84
C-59	29.0	1.75	1.90	5.24	6.18	G-11	55.0	4.16	4.25	3.77	3.93
C-60	30.0	1.78	1.98	5.16	6.39	E-30	56.0	4.07	4.15	4.10	4.26
I-22	32.0	2.01	2.02	5.30	5.35	I-39	56.0	4.27	4.35	3.73	3.87
I-23	33.0	2.06	2.11	5.50	5.77	I-31	56.0	4.03	4.29	3.83	4.34
C-46	33.0	2.28	2.50	3.92	5.06	C-21	57.0	4.29	4.31	3.84	3.97
I-24	34.0	2.05	2.09	5.96	6.19	C-33	57.0	4.30	4.35	3.73	3.95
C-54	37.0	2.46	2.70	4.22	5.09	E-23	57.0	4.26	4.42	3.74	4.03
C-52	38.0	2.75	2.80	4.14	4.30	E-21	57.0	4.30	4.32	3.92	3.95
C-51	40.0	2.45	3.05	3.87	6.00	C-22	57.0	4.29	4.48	3.71	3.97
C-51	40.0	2.60	2.85	4.43	5.32	C-20	57.5	4.30	4.46	3.74	4.02
C-20	40.0	2.90	2.92	4.22	4.28	C-35	58.0	4.42	4.49	3.75	3.87
C-	40.0	2.83	2.85	4.43	4.50	I-38	58.5	4.48	4.55	3.72	3.84
C-	42.5	3.10	3.26	5.82	4.23	I-55	59.0	4.55	4.57	3.75	3.78
C-49	42.5	3.23	3.46	3.40	3.90	I-13	59.0	4.50	4.52	3.83	3.87
C-44	43.5	3.16	3.26	4.00	4.26	I-17	60.0	4.11	4.31	4.36	4.80
C-57	44.0	3.18	3.20	4.25	4.31	C-34	60.5	4.68	4.71	3.71	3.76
C-55	45.4	3.22	3.25	4.31	4.39	E-22	61.0	4.66	4.67	5.84	3.86
G-25	45.0	3.05	3.15	4.10	4.90	C-37	61.0	4.70	4.76	3.70	3.79
C-45	45.0	3.30	3.33	4.39	4.18	C-38	61.0	4.97	5.13	3.18	3.39
I-25	45.0	3.62	3.76	3.22	3.48	C-24	61.0	4.70	4.88	3.57	3.79
C-53	45.0	3.31	3.34	4.08	4.16	C-10	61.0	4.63	4.76	3.70	3.91
I-29	45.0	3.57	3.61	3.50	3.58	I-40	61.5	4.78	4.80	3.69	3.72
C-56	46.5	3.35	3.40	4.21	4.34	C-40	62.0	4.90	4.92	3.57	3.60
C-65	46.5	3.27	3.33	4.39	4.55	G-39	62.0	5.06	5.15	3.26	3.38
C-43	47.0	3.51	3.56	3.92	4.03	E-38	62.0	4.19	4.22	4.86	4.93
G-33	47.0	3.35	3.55	3.94	4.43	G-38	63.0	4.68	4.70	4.04	4.08
I-18	47.0	3.50	3.66	3.71	4.06	C-19	64.0	4.98	5.00	3.69	3.72
G-26	47.5	3.35	3.48	4.19	4.52	I-36	64.0	4.94	5.01	3.67	3.78
G-21	48.5	3.46	3.58	4.13	4.42	C-9	65.0	5.06	5.26	3.44	3.71
E-26	49.0	3.51	3.59	4.19	4.38	C-4	65.0	5.05	5.50	3.14	3.72
E-19	49.0	3.37	3.63	4.10	4.76	I-41	65.0	4.91	4.94	3.90	3.94
I-12	49.5	3.70	4.05	3.36	4.03	E-40	66.0	5.60	5.62	3.10	3.12
G-17	50.0	3.55	3.78	3.94	4.46	C-7	67.0	5.08	5.30	3.60	3.91
G-18	50.0	3.75	3.77	3.96	4.00	C-18	68.0	5.49	5.52	3.41	3.45
G-19	50.0	3.95	3.97	3.57	3.60	I-37	68.0	5.37	5.39	3.58	3.61
E-27	50.5	3.79	3.82	3.93	4.00	C-23	68.5	5.44	5.44	3.57	3.57
I-31	51.0	3.76	4.00	3.66	4.14	C-17	69.0	5.41	5.44	3.62	3.66
G-34	51.0	3.88	3.92	3.81	3.89	C-15	69.0	5.32	5.51	3.53	3.78
C-31	51.5	3.85	3.91	3.90	4.03	C-16	69.0	5.51	5.52	3.52	3.53
C-28	52.0	3.83	4.04	3.73	4.15	C-8	69.0	5.44	5.46	3.59	3.62
E-24	52.0	3.82	3.93	3.94	4.17	G-41	70.0	5.30	5.33	3.88	3.92
G-20	52.0	3.90	3.92	3.96	4.00	C-6	71.0	5.50	5.53	3.71	3.75
C-28	52.0	3.89	3.91	3.98	4.02	C-11	72.5	6.16	6.18	3.10	3.12
C-30	52.0	3.93	3.95	4.05	3.94	C-14	73.0	5.66	5.67	3.73	3.74
I-32	52.0	3.97	4.00	3.96	3.86	E-36	73.0	5.75	5.78	3.59	3.63
E-20	52.0	3.89	3.92	3.96	4.02	G-12	74.0	5.76	5.77	3.70	3.71
C-29	53.0	3.93	3.97	4.01	4.09	C-1	75.0	6.19	6.27	3.22	3.30
C-27	53.0	3.83	3.98	3.84	4.31	C-35	75.0	5.96	5.99	3.34	3.56
C-26	53.0	3.90	4.03	3.96	4.16	C-36	75.5	6.15	6.20	3.34	3.39
C-42	53.0	4.07	4.09	3.78	3.82	C-13	79.0	6.15	6.16	3.70	3.71
C-41	53.5	4.04	4.08	3.87	3.95	E-11	79.5	6.64	6.71	3.16	3.22
C-32	54.0	3.93	4.18	3.76	4.25	C-39	80.0	6.22	6.24	3.70	3.72
E-18	54.5	4.17	4.27	3.66	3.84	E-13	82.5	6.44	6.58	3.54	3.69
E-31	55.0	3.69	4.18	3.90	5.00	C-12	83.0	6.52	6.72	3.43	3.65
						E-12	91.0	7.15	7.32	3.48	3.64

a. 1985 data obtained with the 80-MHz antenna.
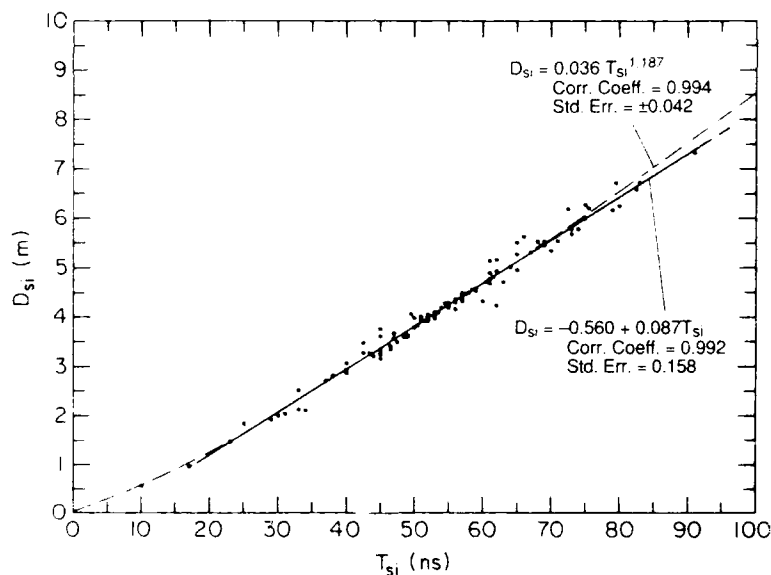
b. 1987 data obtained with the 120-MHz antenna.

Figure 4. Snow and ice thickness, D_{si}, vs two-way EM wavelet flight time, T_{si}, in snow and ice.
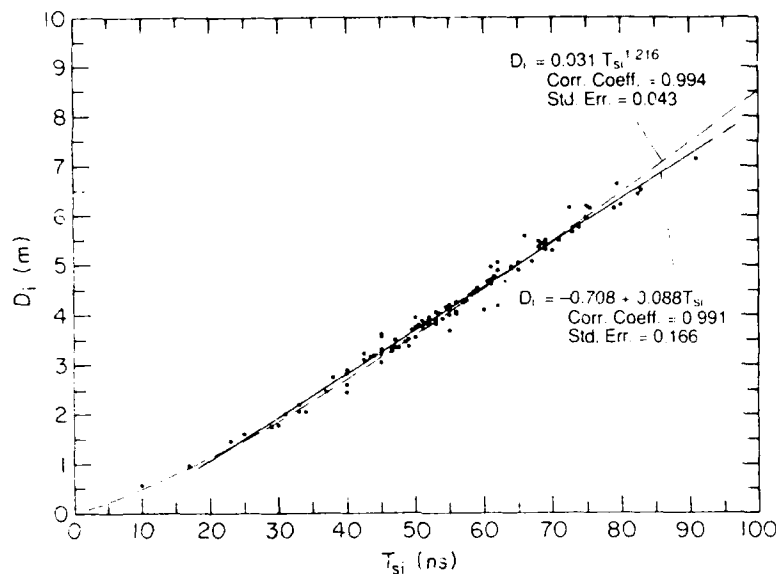
7

Figure 5. Ice thickness, D_i, vs two-way EM wavelet flight time, T_{si}, in snow and ice for 1987 data obtained with the 120-MHz antenna.

snow cover thickness (averaging 20 cm in 1985 vs 11 cm in 1987) and, to a lesser extent, to antenna frequency and timing variations between antennas, and to ice floe property variations.
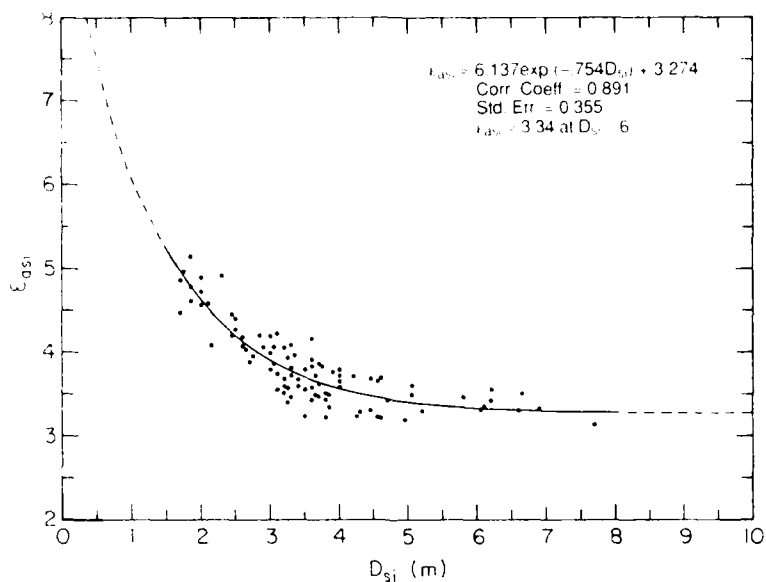
For the situation where only sea ice thickness is desired, we stripped out the snow thickness and provide the relation between D_i and T_{si} for the 1987 data in Figure 5. This relation may be useful for estimating the relative thickness of cold winter sea ice between about 1 and 8 m thick.

Plots of E_{asi} as a function of D_{si} for the 1985 and 1987 data are given in Figure 6. A similar plot of E_{ai} vs D_i for the 1987 data is shown in Figure 7. These plots clearly show that E_{asi} and E_{ai} increase rapidly with decreasing ice thickness. This is expected since the brine content is higher in the thinner ice and it is this conductive liquid fraction that greatly affects the electromagnetic properties of sea ice (Kovacs et al. 1987). As sea ice grows thicker and ages, more brine will drain out of the ice. The result is that the bulk dielectric constant of the thicker ice
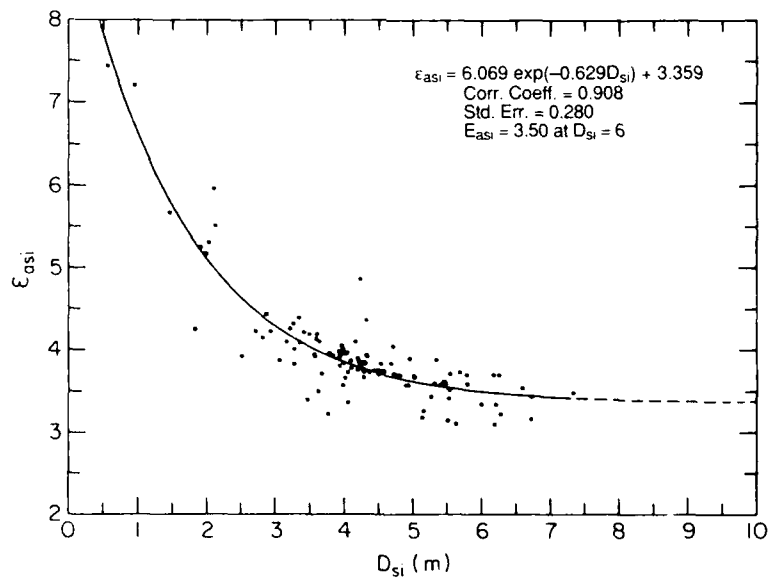
seems to reach a relative constant value, as can be inferred from the data in Figure 6. This trend is in agreement with the model results of Kovacs et al. (1987).

Our attempt to profile the snow–ice thickness from the air at the 1985 field site was not successful. An attempt by Exxon Corporation, using a radar system developed for them by Cambridge Consultants, Ltd., Cambridge, England, to profile the same floe was also not successful.[*] We believe the ice was too lossy to allow the 80-MHz antenna's transmitted EM wavelet to penetrate to and be reflected from the bottom of this type of sea ice. This was so even when the helicopter-mounted antenna was flown as low as 5 m above the surface. No airborne radar profiling was undertaken during the 1987 field study.

---

[*] Personal communication with G.F. Gehrig, Exxon Production Research Company, Houston, Texas, 1989.

$\varepsilon_{asi} = 6.137 \exp(-.754D_{si}) + 3.274$
Corr. Coeff. $= 0.891$
Std. Err. $= 0.355$
$\varepsilon_{asi} = 3.34$ at $D_{si} = 6$

a. 1985 data obtained with the 80-MHz antenna.

$\varepsilon_{asi} = 6.069 \exp(-0.629D_{si}) + 3.359$
Corr. Coeff. $= 0.908$
Std. Err. $= 0.280$
$E_{asi} = 3.50$ at $D_{si} = 6$

b. 1987 data obtained with the 120-MHz antenna.

Figure 6. Apparent dielectric constant of snow and ice, E_{asi}, vs snow and ice thickness, D_{si}.
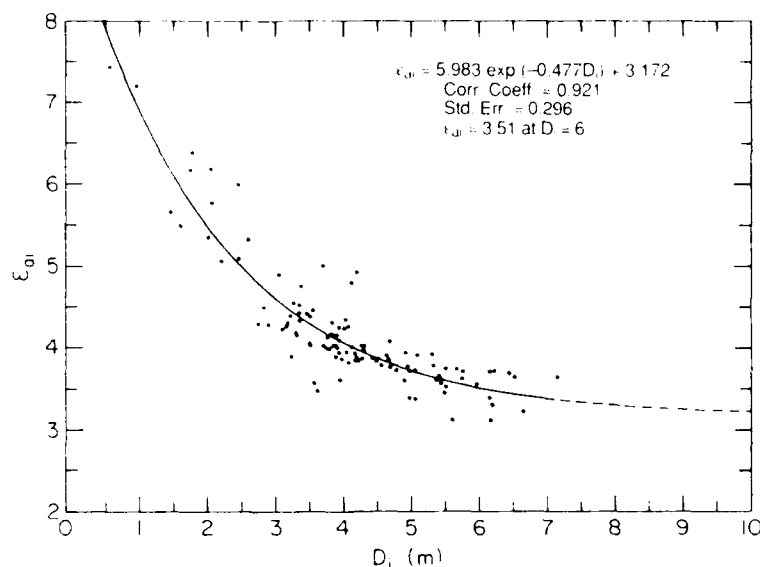
Figure 7. Relative apparent dielectric constant for ice, E_{ai}, vs ice thickness, D_i, for 1987 data obtained with the 120-MHz antenna.

DISCUSSION

The data presented in this report allowed development of relationships for estimating snow plus sea ice thickness and ice thickness from just the measured two-way time-of-flight of an EM wavelet, in about the 100- to 200-MHz frequency band, traveling from the surface to the ice "bottom" and back to the surface. Knowledge of the bulk dielectric constant or the EM wavelet velocity in the snow and ice is not needed. The simple linear relationships seem to be good for ice thickness from about 1 to 8 m. Another relationship presented is that found between E_{ai} and D_i. This relation shows that thin winter sea ice has a higher E_{ai} than thick ice. This is reasonable since the dielectric constant of pure ice, at the frequencies of interest, is about 3.15, but for sea ice the bulk dielectric constant is higher (because of its brine content) and varies with brine volume. However, as sea ice grows thicker or ages, there is less brine in the ice because of brine drainage processes. This drainage "freshens" the ice and, thus, reduces its bulk dielectric constant.

LITERATURE CITED

Kovacs, A., R.M. Morey, G.F.N. Cox (1987) Modeling the electromagnetic property trends in sea ice, Part I. *Cold Regions Science and Technology*, **14**: 207–235.

10

A facsimile catalog card in Library of Congress MARC format is reproduced below.

Kovacs, Austin
   Estimating sea ice thickness using time-of-flight data from impulse radar soundings / by Austin Kovacs and Rexford M. Morey. Hanover, N.H.: U.S. Army Cold Regions Research and Engineering Laboratory; Springfield, Va.: available from National Technical Information Service, 1989.
   ii, 13 p., illus., 28 cm. (CRREL Report 89-22.)
   Bibliograpl.y: p. 10.
   1. Field studies. 2. Impulse radar soundings. 3. Radar. 4. Sea ice. 5. Sea ice thickness. I. Morey, Rexford M. II. United States Army. III. Corps of Engineers. IV. Cold Regions Research and Engineering Laboratory. V. Series: CRREL Report 89-22.